LOW TEMPERATURE SYNTHESIS AND CHARACTERIZATION OF BISMUTH FERRITE ($Bi_2Fe_4O_9$) NANOPARTICLES BY USING HYDROTHERMAL METHOD

S. ALTAF[a], K. ALI*[a], H. M. KHAN[b], K. SARDAR[a], K. KAMRAN[a], M. A. RAZA[a]

[a]Nano-optoelectronics Research Laboratory, Department of Physics, University of Agriculture Faisalabad, 38040 Faisalabad, Pakistan
[b]Department of Physics, The Islamia University of Bahawalpur, Bahawalpur

$Bi_2Fe_4O_9$ (BFO) is a promising inorganic material having a perovskite structure. The study demonstrated the Preparation of $Bi_2Fe_4O_9$ nanoparticles by hydrothermal method at low temperature. The influence of alkali concentration on BFO was also investigated. The high alkali concentration of the Na^+ ions had a vital role in the production of the bismuth ferrite nanoparticles at low Temperature. Pure BFO nanoparticles were obtained by high alkali concentration. The $Bi_2Fe_4O_9$ nanoparticles thus formed were then characterized by the aid of   Scanning Electron Microscopy (SEM) and X-ray Diffraction (XRD) analysis. UV spectroscopy was performed to study the absorption spectrum and band gap was calculated. XRD described the entire crystal structure of the prepared nanoparticles. The average size of prepared nanoparticles found to be decrease by increasing the concentrations of the initial precursors. The observed peaks have shown perovskite orthorhombic structure and belongs to space group pbam The SEM was performed to study the composition and morphology of the nano particles an well agglomerated and flower like nanoparticles were obtained.

1. Introduction

Bismuth ferrite is among the excellent multiferroic materials synthesized in 1957 for the first time. It has a perovskite structure which is distorted rhombohedrally. Bismuth ferrite possess a high Curie temperature (T_C = 1103K). It is another property of bismuth ferrite to possess Neel temperature (T_N = 643K) (Shami *et al.*, 2011). The importance of bismuth ferrite does not lie in its Neel temperature as well as high Curie temperature but it is important due to its ferromagnetic properties at room temperature. To synthesize BFO in single phase is very difficult as it possess a very narrow range of temperature stability (Texas *et al.*, 2017).

Bismuth ferrite is very important among the other iron oxides with orthorhombic structure. The magnetic properties of bismuth ferrite are dependent on its chemical composition. Its applications are very vast and now a day it is used as an important material in electrochemical sensors, lithium ion batteries and field emissions (Manar, 2016). The orthorhombic $Bi_2Fe_4O_9$ is very interesting material with its photocatalytic applications. The photochemical applications involve the use of $Bi_2Fe_4O_9$ in the form of nanowires and nanosheets (Zhao *et al.*, 2011a).

To synthesize single crystalline $Bi_2Fe_4O_9$ cubes and nano wires, molten salt method and template induced sol-gel route have been successfully used. A very high temperature is still required (>800˚C) for the synthesis. Hydrothermal is one of the most important methods for the synthesis of $Bi_2Fe_4O_9$ nanoparticles(Wang *et al.*, 2009a). This method is cost effective and provides well controlled morphology of nanoparticles.

_____
*Corresponding author: khuram_uaf@yahoo.com

The previous work on hydrothermal synthesis shows that temperature required for it must be greater than 180˚C. It is aim of a many researcher to obtain ultrafine $Bi_2Fe_4O_9$ nanopowders under suitable conditions using hydrothermal method. A lower temperature is required to synthesize ultrafine $Bi_2Fe_4O_9$ nanoparticles (Wang *et al.*, 2009b).

Bismuth ferrite can be synthesized by different methods which involve Sol-Gel, Hydrothermal, Microwave hydrothermal and other synthetic methods. Bismuth Ferrite is prepared easily by using Sol-Gel method. Good crystalline form of BFO is obtained by this method because uniform composition of particles obtained at molecular level at low synthetic temperature (Kumar *et al.*, 2008). Hydrothermal method is also used by many researchers for the synthesis of Bismuth Ferrite. In advance material synthesis hydrothermal technique is one of the important techniques because nanohybrids and nanocomposites can be efficiently prepared using this method (Zhang and Kajiyoshi, 2010). The mechanism of the method involves the dissolution of those materials which are insoluble under ordinary conditions. Using this technique they are made soluble under high temperature and pressure. The reaction is carried out in a Teflon sealed autoclave and then sealed and maintained at a required temperature (Gheorghiu *et al.*, 2013).

The Hydrothermal method is very useful to synthesize the crystalline phases of bismuth ferrite which show zero stability at their melting point. This is the advantage of hydrothermal method among the other synthesizing methods. This method is also used for the synthesis of such materials which show very high vapor pressure. This vapor pressure is found to be close to their melting points. The crystals thus formed by this method are found to be large in size and having a good quality. The composition of the prepared nanoparticles can be controlled by hydrothermal method (Byrappa and Adschiri, 2007).

As compared to Sol-Gel process the BFO is synthesized at a relatively low temperature by hydrothermal method. Another advantage of this method over Sol-Gel is that it helps to control the morphology and size of the BFO nanoparticles more effectively. radiation (Thos et al., 2015). Microwave hydrothermal method is another method for the synthesis of Bismuth Ferrite. In this method heat is introduced through a microwave furnace into the hydrothermal method. It crystallizes the BFO nanoparticles more effectively than the hydrothermal method and reduces the reaction

2. Experimental

$Bi_2Fe_4O_9$ nanoparticles were prepared using hydrothermal method. The chemicals which were used in this synthesis method were bismuth nitrate [$Bi(NO_3)_3.5H_2O$], iron nitrate [$Fe(NO_3)_3.9H_2O$] , Potassium Hydroxide (KOH) and Sodium Hydroxide (NaOH). The bismuth nitrate and iron nitrate were the initial precursors for this synthesis. These chemicals were used as purchased without any purification.

Diluted HNO_3 is taken and initial precursors were dissolved in it. The chemicals were mixed together to form an aqueous solution. The addition of KOH helped to maintain the pH value up to 8 in the aqueous solution. This solution was constantly mixed until formation of brown precipitate. The filtration process was carried out to filter the K^+ and NO_3^- ions from the precipitate. The brown precipitate was mixed with NaOH solution. This mixture was constantly stirred for 5 minutes by a magnetic stirrer. Solution was placed in an autoclave and sealed properly. The hydrothermal treatment was given to the autoclave by placing it in an electric oven. Temperature of the electric oven was maintained at 100˚C for 9 hours. After this hydrothermal treatment the autoclave is removed from the oven and cooled at room temperature. The Products were filtered washed and with the ethanol and distilled water for two to three times. The products were then removed from filter paper very carefully and then dried in an electric oven for 4 hours. The temperature required for drying process ranges between 70 to 80 ˚C (Wang *et al.*, 2009b).

XRD and SEM were used to characterize the prepared samples. XRD analysis was performed to understand and examine the external structu.re of the prepared nanoparticles. SEM was used further to study the morphology of the nanoparticles (Zhang *et al.*, 2011). UV specroscopy was performed to obtain the absorption spectrum. The band gap was calculated from the absorbtion spectrum (Xu *et al.*, 2016).

3. Results and discussion

3.1. XRD analysis

The Fig. 3.1 showed the diffraction pattern for different concentrations of the bismuth nitrate and iron nitrate respectively and indicates the considerable peaks. These peaks were indexed according to the standard pattern of the orthorhombic phase of the $Bi_2Fe_4O_9$ as shown in Figure 1. The characteristic peak for the sample was observed on the plane 121 which would be relatable with the standard pattern of the $Bi_2Fe_4O_9$ (Yang *et al.*, 2017). The alkali concentration of 5 moles helped to prevent the $BiFeO_3$ phase. Below this concentration the $BiFeO_3$ peaks might be observed but at 5 mol or greater, the pure $Bi_2Fe_4O_9$ phase was obtained. The peaks were indexed according to the standard pattern of the orthorhombic $Bi_2Fe_4O_9$ nanoparticles (Park *et al.*, 2005).
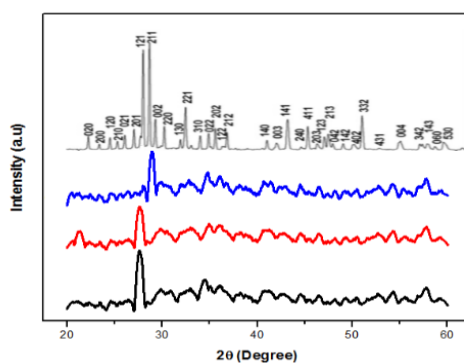

Fig. 1. X-Ray Diffraction patterns of $Bi_2Fe_4O_9$ nanoparticles with alkali concentration maintained at 5 moles and different initial precursor concentrations (a) 0.09 M and 0.18 M (b) 0.11 M and 0.22 M (c) 0.14 and 0.18 M.

The observed peaks have shown perovskite orthorhombic structure and they were wide also which confirmed the pure structure of the $Bi_2Fe_4O_9$. The characteristic peak possessed all the important properties of the material. It was observed that by increasing the concentrations of the initial precursors the number of peaks also increased. This also means that the crystallization was occurred more efficiently. After comparing the peaks of different samples it was concluded that with the increase in precursor amount the crystallization process is enhanced. The concentrations of bismuth nitrate and iron nitrate were also a contributing factor for the crystallization. The number of peaks obtained from X-Ray diffraction analysis showed that by increasing initial concentrations of the precursors the number of peaks also increased. The increased concentration of the precursor provided more reaction sites which further helped in the crystallization process. The average particle size calculated is given below.

Table 1. Average Particle size of Samples of different concentrations at $100^{\circ}C$.

Serial No	Temperature (degree Celsius)	Concentration of Initial Precursors		Average particle size(nm)
		$Fe(NO_3)_3.9H_2O$ (mol)	$Bi(NO_3)_3.5H_2O$ (mol)	
1	100	0.18	0.09	4.1898
2	100	0.22	0.11	3.9056
3	100	0.28	0.14	3.6943

The obtained results were compared with the work of other researchers and it was concluded that the peaks were slightly shifted from the reference data (Xiong *et al.*, 2004). This

happened probably because the concentrations of the initial precursors were different for each sample.

3.2. Morphological analysis

Figure 2 exhibits the scanning electron microscopy of the prepared samples. SEM was performed with suitable voltage to study the morphology of the prepared samples.
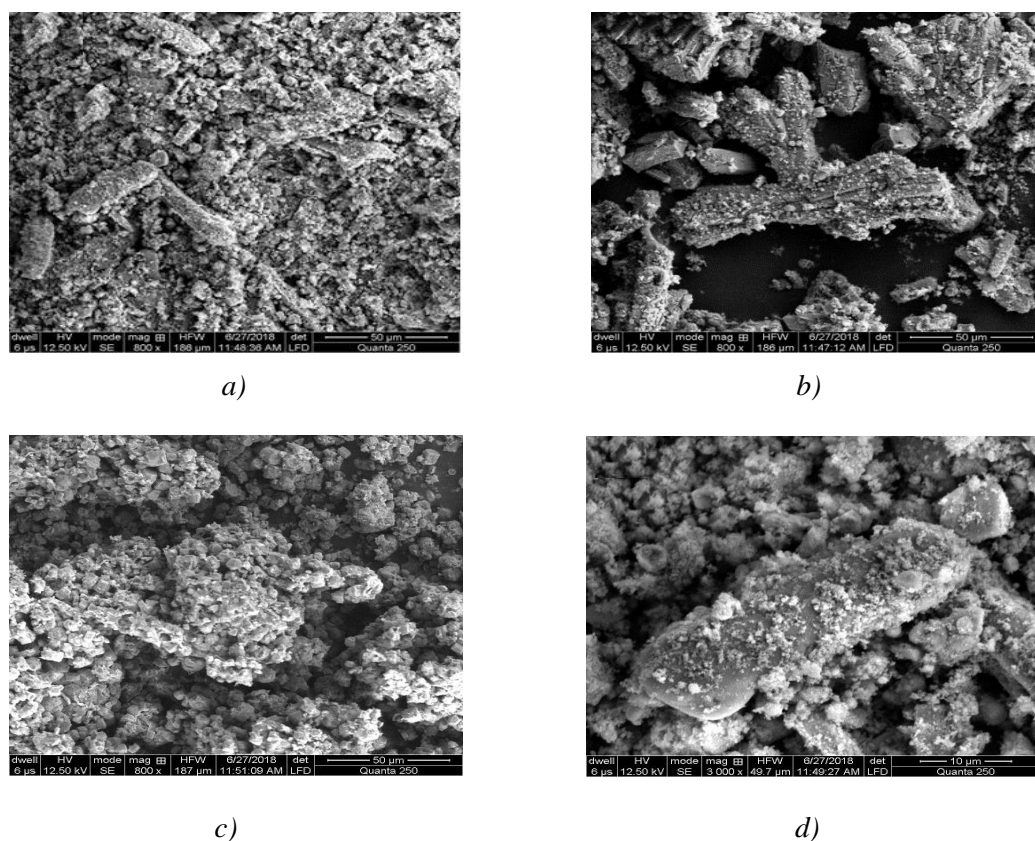

a)   *b)*

c)   *d)*

Fig. 2. SEM of $Bi_2Fe_4O_9$ nano particles with alkali concentration maintained at 5 moles and different initial precursor concentrations (a) 0.09 M and 0.18 M (b) 0.11 M and 0.22 M (c) 0.14 and 0.18 M at 800x (d)) 0.09 M and 0.18 M at 3000x.

The Scanning Electron Microscopy revealed the information about the morphology of the $Bi_2Fe_4O_9$ nanoparticles with narrow size distribution. The alkali concentration was maintained at 5 moles for all the samples to obtain this phase of Bismuth Ferrite. The figure described that the samples were found to be well agglomerate. The low temperature of the reaction also contributed towards crystallization. SEM reveals that the crystals of the $Bi_2Fe_4O_9$ were controlled by anisotropy of the intrinsic crystal structure. As a result of this the $Bi_2Fe_4O_9$ crystals grow and then agglomerate (Park *et al.*, 2005). This also promotes the growth and agglomeration of the particles in a specific direction. These crystals were found to be well dispersed. The cubic shape of the co existing particles was observed in the Figure 2 (d). These results agreed with research work performed by other researchers (Liu and Zuo, 2013). The thickness of the nanoparticles was depended on the NaOH concentration. The alkali concentration was kept constant. In Figure 2(b) the analysis from Scanning Electron Microscopy revealed the flower like morphology. The low temperature of the reaction also contributed towards crystallization.

3.3. UV Spectroscopy

The prepared samples were characterized by UV spectroscopy to study the absorbance of the samples. The bandgap was calculated by the aid of absorbance data. There are certain methods to calculate band gap but in this literature Tauc plot method is discussed shortly. (Hasan *et al.*,

n.d.). The bandgap was calculated with the help of Tauc and Davis Mott relation. The equation is as follows

$$(\alpha h \nu)^n = k (h \nu - E_g)$$

In this relation n is taken as 2 showed the nature of the transition. Bismuth Ferrite is a material with direct band gap. The $h\nu$ indicated the incident photon energy and k is energy independent co-efficient. E_g denoted the optical bandgap. The α is absorption Co-efficient and was calculated by using Beer lambert law. The calculated value of α is 2.303 A cm-1 (Godara *et al.*, 2014). The figures exhibited the absorption spectrum of $Bi_2Fe_4O_9$ nanoparticles.
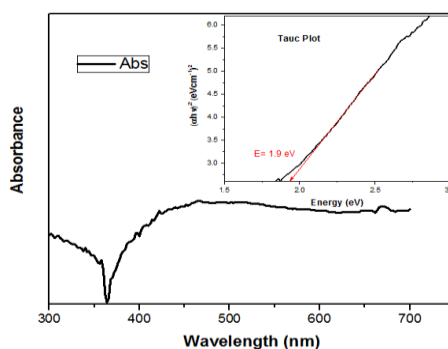

Fig. 3. UV-Visible optical absorption spectrum and calculated Band gap Eg =1.9 eV.

It was obtained from Fig. 3.3 that the bismuth ferrite nanoparticles have showed strong absorption. The wavelength corresponding to this absorption ranges between 350-550 nm. The wavelength range from 550-700 nm have showed the slight absorption. The E_g = 1.9 eV was obtained by the Tauc plot method as shown in Figure 3. The band gap had same value near to as reported in the literature cited (Zhao *et al.*, 2011b).
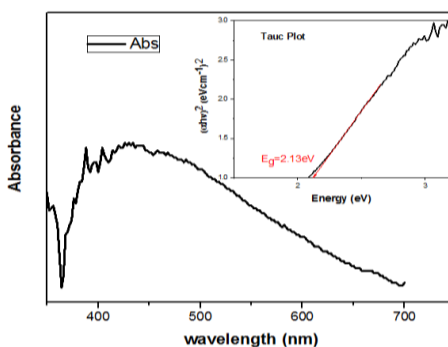

Fig. 4. UV-Visible optical absorption spectrum and calculated Band gap Eg =2.13 eV.

Figure 4 exhibited the Absorbance spectrum and bandgap for the sample with a greater concentration of initial precursors as compared to the Figure 3. The figure exhibited the strong absorption from 400-500 nm. The band gap was 2.13 eV which agreed with the results previously obtained (Mukherjee *et al.*, 2012). The band gap was slightly increased with a further increase in the concentration of the initial precursors as shown in Figure 5.
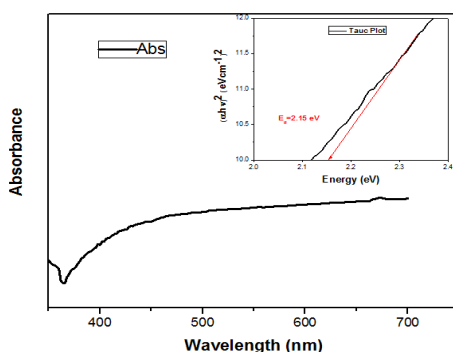
Fig. 5. UV-Visible optical absorption spectrum and calculated Band gap Eg =2.15 eV.

The range for strong absorption had shown in Figure 4. The E_g of 2.15 eV was obtained from the plot which agreed with the previous literature (Cho *et al.*, 2008).

4. Conclusion

$Bi_2Fe_4O_9$ nanoparticles were efficiently prepared by the aid of hydrothermal method at a very low temperature of 100˚C. This low temperature was adequate because of the high alkali concentration. The pure phase of BFO was obtained due to the alkali cations. The size of the nanoparticles was decreased by increasing the concentrations of the initial precursors. XRD had described the entire crystal structure of the prepared nanoparticles. The observed peaks had shown perovskite orthorhombic structure and belong to pbam space group. The SEM was performed to study the composition and morphology of the nano particles. Well agglomerated and flower like nanoparticles were obtained from SEM at a low temperature. The optical study of the prepared samples were performed to calculate the bandgap. It is well reasoned that some other nano particles can also be prepared by the Hydrothermal method which include Manganese Zinc ferrites, Nickel Zinc Ferrites and many more under milder conditions.

Acknowledgement

References

[1] K. Byrappa, T. Adschiri, Progress in Crystal Growth and Characterization of Materials **53**(2), 117 (2007).
[2] C. M. Cho, J. H. Noh, I. S. Cho, J. S. An, K. S. Hong, J. Y. Kim, Journal of the American Ceramic Society **91**(11), 3753 (2008).
[3] F. Gheorghiu, R. Tanasa, M. T. Buscaglia, V. Buscaglia, C. G. Pastravanu, E. Popovici, L. Mitoseriu, Phase Transitions **86**(7), 726 (2013).
[4] S. Ghosh, S. Dasgupta, A. Sen, H. S. Maiti, Journal of the American Ceramic Society **88**(5), 1349 (2005).
[5] S. Godara, N. Sinha, G. Ray, B. Kumar, Integrative Medicine Research, 1 (2014).
[6] M. Hasan, M. A. Basith, M. A. Zubair, S. Hossain, R. Mahbub, (n.d.) Saturation magnetization and band gap tuning in $BiFeO_3$ nanoparticles via co – substitution of Gd and Mn 3.

[7] M. Kumar, K. L. Yadav, G. D. Varma, Materials Letters **62**(8-9), 1159 (2008).

[8] Y. Liu, R. Zuo, Particuology **11**(5), 581 (2013).

[9] T. El. Manar, Optimization of the synthesis of multiferroic bismuth ferrite $BiFeO_3$ nanopowders by hydrothermal method (January), 2016.

[10] A. Mukherjee, M. Pal, C. Glass, S. Basu, Effect of Y-doping on optical properties of multiferroics BiFeO3 nanoparticles Effect of Y-doping on optical properties of multiferroics (September), 2012.

[11] T.-J. Park, G. C. Papaefthymiou, A. R. Moodenbaugh, Y. Mao, S. S. Wong, Journal of Materials Chemistry **15**(21), 2099 (2005).

[12] M. Y. Shami, M. S. Awan, M. Anis-Ur-Rehman, Journal of Alloys and Compounds **509**(41), 10139 (2011).

[13] M. R. Texas, T. Nanostructures, R. E. Sources, P. View, Spark plasma sintering of hydrothermally synthesized bismuth ferrite (January 2016), 257 (2017).

[14] E. Thos, L. Ogos, P. Athos, Three Methods of Persuasion **7**(4), 165 (2015).

[15] Y. Wang, G. Xu, L. Yang, Z. Ren, X. Wei, W. Weng, P. Du, G. Shen, G. Han, Ceramics International **35**(3), 1285 (2009).

[16] Y. Wang, G. Xu, L. Yang, Z. Ren, X. Wei, W. Weng, P. Du, G. Shen, G. Han, Ceramics International **35**(1), 51 (2009).

[17] Xiong, Y., M. Wu, Z. Peng, N. Jiang, Q. Chen, Chemistry Letters **33**(5), 502 (2004).

[18] H. Xu, H. Wang, J. Shi, Y. Lin, C. Nan, Heterostructured Thin Films, 1 (2016).

[19] H. Yang, J. Dai, L. Wang, Y. Lin, F. Wang, P. Kang, Scientific Reports **7**(1), 768 (2017).

[20] H. Zhang, K. Kajiyoshi, Journal of the American Ceramic Society **93**(11), 3842 (2010).

[21] J. Zhao, T. Liu, Y. Xu, Y. He, W. Chen, Materials Chemistry and Physics **128**(3), 388 (2011).